Free-Space Optical Communication Impaired by Angular Fluctuations

Free-Space Optical Communication Impaired by Angular Fluctuations

Shenjie Huang, *Student Member, IEEE,* Majid Safari, *Member, IEEE*

***Abstract*—In this paper, the impairments of FSO communication systems caused by angular fluctuations including beam misalignment and angle-of-arrival (AOA) fluctuations are modelled in the presence of both atmospheric turbulence and transceiver vibrations. In particular, assuming FSO receivers with a limited field-of-view (FOV), the fading caused by AOA fluctuations is studied. The outage probability expressions for both coherent and direct detections are derived in both shot-noise-limited and thermal-noise-limited regimes. For direct detection, the optimal receiver FOV that achieves the minimum outage probability is considered. Furthermore, the issue of imperfect phasefront tracking in practical coherent receivers is investigated.**

***Index Terms*—Free-space optical communication, angular fluctuations, transceiver vibrations, pointing error, angle of arrival, building sways, coherent detection, atmospheric turbulence, outage probability.**

I. Introduction

The scarcity in the radio frequency spectrum has now become the primary limitation to the expansion of wireless communication networks. As a potential candidate for long-range wireless connectivity in future networks, free-space optical (FSO) communication is attracting more and more attention by researchers because of high achievable data rates, license-free spectrum, outstanding security level and low installation cost [1]. Terrestrial FSO links can be used to extend backhaul and last mile connectivities in future 5G networks. However, as a line-of-sight communication technology, the application of FSO systems are limited by a number of impairments caused by atmospheric turbulence such as fluctuations in both intensity and phase, beam spread and angular spread [2].

A number of techniques have been proposed to mitigate turbulence-induced intensity fluctuations [3]–[9]. Spatial diversity is an attractive approach and substantial performance gain can be achieved by using direct detection with spatial diversity at both transmitter and receiver sides [3]. In [4], MIMO FSO systems are investigated in the presence of correlation among multiple turbulent fading channels. Distributed MIMO and relay-assisted systems are also considered in FSO to improve the performance of long-range FSO links [5], [6]. Besides employing multiple receivers, a single large aperture can also be used to reduce the intensity fluctuations due to the aperture averaging [7]. The effect of link geometry on the diversity and multiplexing gain of a multi-beam FSO system is investigated in [8]. Moreover, in [9], an adaptive array receiver is employed to enlarge the receiver field-of-view (FOV) as well as to reduce the amount of background noise collected by the receiver.

All of the aforementioned works considered intensity modulation with direct detection (IM/DD) which is the most common technique because of its simplicity. However, direct detection may not be able to provide sufficient receiver sensitivity for adverse channel conditions where the signal is swamped by shot noise and thermal noise. Because of its noise rejection capability, coherent detection has been applied as a method of enhancing the FSO system performance [1]. Lee *et al.* have addressed the benefits of coherent detection with spatial diversity over direct detection in a shot-noise limited regime [10]. However, the performance of coherent detection can be significantly degraded by turbulence-induced phase distortion. The impact of atmospheric phase distortion to the coherent detection has been thoroughly analysed and some techniques have been proposed to mitigate the induced degradation such as modal phase compensation [11] and wavefront predistortion [12]. However, these phase compensation techniques substantially increase the complexity of the practical FSO communication system. Nevertheless, a practical coherent FSO receiver can be realised by reducing the diameter of the receive aperture below the coherence length of the turbulence thereby only requiring to compensate for the phase distortions of one spatial mode. In this paper, we compare the performance of such practical coherent FSO receivers with more commonly used direct detection receivers in the presence of angular fluctuations including the effects of both random beam misalignment and angle-of-arrival (AOA) fluctuations.

AOA fluctuations at the receiver lead to image dancing (jitter) on the focal plane which can attenuate the received power for the receivers with limited FOV [2]. However, most of the works in the literature focusing on terrestrial FSO communication only consider receivers with very large FOV thereby neglecting the effects of AOA fluctuations [13], [14]. Larger FOV implies a larger received background radiation which could significantly degrade the system performance [15]. Furthermore, practical high-speed FSO systems typically employ small photodetectors which can provide wide electrical bandwidth leading to a limited receiver FOV that can also reduce the effect of ambient light [16]. The statistical characteristics of turbulence induced AOA fluctuations has been derived in many works [2], [17], [18] and AOA compensation methods have also been investigated [19], [20]. However, the effect of fading caused by AOA fluctuations on terrestrial FSO communication systems has not been comprehensively investigated in the literature. In our previous work, the impacts of turbulence-induced AOA fluctuations on the performance of practical FSO communication systems employing receivers with limited FOV are investigated [21]. However, the simple model proposed in [21] cannot describe the system performance precisely especially in high transmit power regime.

The alignment between transmitter and receiver are critical for FSO systems. However, this alignment can be destroyed by transceiver vibrations caused by effects such as building sways occur in both transmitter and receiver sides [13]. Beam misalignment fading due to pointing errors caused by transmitter vibrations has been investigated in a number of studies [22]–[24]. Under the assumption that the receiver aperture size is very small compared to the beam size on the receiver plane, the fading caused by beam misalignment can be modelled as beta distribution [22], [23]. A more accurate fading model considering the receiver aperture size is proposed in [24] which is applicable in all ranges of FSO links. This model has been applied in many works to investigate the effect of beam misalignment on different optical communication systems such as MIMO [25] and coherent [26] FSO systems. More recently the capacity of FSO links in the presence of generalized beam misalignment is analysed [27], [28]. Besides beam misalignment caused by transmitter vibrations, the receiver vibrations affect the FSO link performance by aggravating AOA fluctuations originally induced by atmospheric turbulence [15], [16]. This effect has been ignored in all of above works by assuming wide receiver FOV.

In this paper, the impairments of terrestrial FSO systems caused by angular fluctuations are modelled taking into account both atmospheric turbulence and transceiver vibrations. In particular, the fading induced by AOA fluctuations is accurately modelled considering both atmospheric turbulence and receiver vibrations. The outage performance of both coherent and direct detection FSO receivers is analyzed in shot-noise and thermal-noise limited regimes. For FSO systems with direct detection in the absence of active tracking subsystems, the optimal size of the receiver FOV which can be achieved numerically is proposed to mitigate the effect of AOA fluctuations. Furthermore, the issue of imperfect phasefront tracking in practical coherent receivers is investigated.

The rest of the paper is organized as follows. In Section II, we describe the channel model that will be used in this paper. In Section III, the outage performance is investigated. The effect of angular fluctuations on coherent detection with imperfect AOA tracking is discussed in Section IV. The thermal-noise-limited analysis is given in Section V. Finally, we conclude this paper in Section VI.

II. Channel Model

In this work, the effects of both turbulence and transceiver vibrations on FSO systems are considered. Turbulence introduces not only log-amplitude fluctuations but also turbulence-induced AOA fluctuations which attenuate the amount of power collected by the photodetector for limited FOV receivers. Transceiver vibrations result in beam misalignment fading as investigated in [24] and also make contributions to AOA fluctuations. A detailed description of these channel impairments will be shown here.

A. Log-Amplitude Fluctuations

Different distributions can be employed to describe turbulence-induced amplitude fluctuations, such as log-normal distribution, K-distribution and gamma-gamma distribution. For FSO systems work under weak turbulence, the amplitude fluctuations are commonly modelled as log-normal distribution [2]. Therefore, the optical signal collected by receive aperture can be expressed as [21]

$$x(\mathbf{r}) = s_r(\mathbf{r})e^{\chi + j\theta(\mathbf{r})}, \tag{1}$$

where $\mathbf{r}$ refers to the position vector on the aperture plane, $s_r(\mathbf{r})$ refers to the signal complex envelope across the receiver aperture which is related to the path loss and beam misalignment, χ is the turbulence-induced log-amplitude fading factor with normal distribution and $\theta(\mathbf{r})$ is the random phase term which results in AOA fluctuations. Note that the time dependence in (1) is dropped for the sake of simplicity. In our communication system, the receiver aperture size is set smaller than the coherence length of the received phasefront so that turbulence-induced amplitude remains unchanged over the aperture [29], [30]. The coherence length r_0 is roughly a measure of the spatial distance between two points in the receiver plane when the optical fields in these two points can be treated as statistically independent. For horizontal links, r_0 is a function of the index-of-refraction structure constant C_n^2 and propagation distance L which is expressed as [2]

$$r_0 = 3.0(C_n^2 L k^2)^{-3/5}, \tag{2}$$

where $k = 2\pi/\lambda$ is the optical wave number. Note that C_n^2 can be regarded as a description of the condition of turbulence. For near ground FSO communication, C_n^2 varies from 10^{-17} $\mathrm{m}^{-2/3}$ for very weak turbulence to 10^{-13} $\mathrm{m}^{-2/3}$ for very strong turbulence [31]. It is noteworthy that in our far-field communication system, in order to mitigate the impairment induced by pointing errors, Gaussian-beam waves with relatively large divergence are employed. For such beams, spherical wave model which is more analytically tractable can be effectively applied as an accurate approximation [7], [32]. Thus when describing the turbulence effects, we will use spherical wave model for simplicity.

In order to ensure that energy conservation is satisfied, we hold $m_\chi = -\sigma_\chi^2$ where m_χ and σ_χ^2 respectively denote the mean and the variance of the log-amplitude fluctuations, χ, introduced in (1). The variance of the log-amplitude fluctuations, σ_χ^2, depends on wave number turbulence condition and propagation length. Assuming that the turbulence is homogeneous and isotropic and the FSO link operates at a weak turbulence condition, σ_χ^2 is given by [2], [21]

$$\sigma_\chi^2 = 0.124 k^{7/6} L^{11/6} C_n^2. \tag{3}$$

The turbulence-induced power fading factor of the received optical field in (1) is denoted as $h_a = e^{2\chi}$ which is log-normal distributed with PDF given by

$$f_{h_a}(h_a) = \frac{1}{2h_a\sqrt{2\pi\sigma_\chi^2}} \mathrm{e}^{\frac{-\left(\ln h_a + 2\sigma_\chi^2\right)^2}{8\sigma_\chi^2}}. \tag{4}$$

Note that the CDF of h_a can then be written as

$$\mathcal{G}(x) = \frac{1}{2}\mathrm{erfc}\left(\frac{-\ln x - 2\sigma_\chi^2}{\sqrt{8}\sigma_\chi}\right), \quad x \in [0, +\infty]. \tag{5}$$

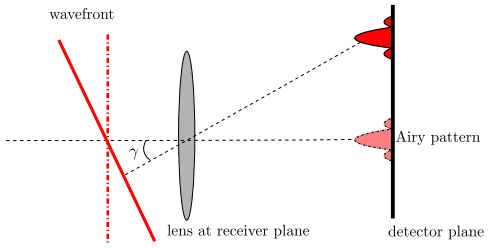

Fig. 1. Angle-of-Arrival fluctuations and diffracted pattern jitter. The red dash-dotted line refers to the wavefront in the absence of AOA fluctuations and the red solid line refers to that with AOA fluctuations.

It is worth mentioning that although this work focuses on weak turbulence regime which has been considered in many works in the literature [6], [24], the derivations and discussions can be readily extended to moderate and strong turbulence scenarios by applying other commonly used scintillation models like gamma-gamma or exponential distributions.

B. Turbulence-Induced Angle-of-Arrival Fluctuations

The atmospheric turbulence causes random phase variation on the transmitted optical wavefront. For a receiver aperture which is small compared to the radius of curvature of the received wavefront, the wavefront across the aperture is essentially a tilted plane [2], [30]. The angle of the wavefront tilted from normal is denoted as the angle-of-arrival at the receiver which results in the jitter of diffraction pattern on the detector plane as shown Fig. 1. The *Turbulence-induced AOA*, γ, is commonly defined as [2], [33]

$$\gamma = \Delta S/(kd), \tag{6}$$

where ΔS is the total phase shift across the aperture, d refers to the diameter of the aperture and k is the optical wave number. The second moment of γ can be written as [33]

$$E[\gamma^2] = \frac{D_S(d,L)}{(kd)^2}, \tag{7}$$

where $D_S(d,L)$ is the phase structure function which is often assumed equal to wave structure function for most engineering applications, i.e., $D_S(d,L) \approx D(d,L)$ [33]. Given the spatial power spectral density, $\Phi_n(\kappa)$, the wave structure function $D(d,L)$ takes the form [2]

$$D(\rho,L) = 8\pi^2 k^2 L \int_0^1 \int_0^\infty \kappa \Phi_n(\kappa)[1 - J_0(\kappa\xi\rho)]\mathrm{d}\kappa\mathrm{d}\xi, \tag{8}$$

where ρ refers to the distance between two observation points, κ is the scalar spatial frequency, and J_0 refers to the bessel function of the first kind and order zero. The spatial power spectral density of the turbulence, $\Phi_n(\kappa)$, can be expressed using the von Kármán spectrum as

$$\Phi_n(\kappa) = \frac{0.033 C_n^2 \exp\left(-\kappa^2/\kappa_m^2\right)}{(\kappa^2 + \kappa_0^2)^{11/6}}, \tag{9}$$

where $\kappa_0 = 2\pi/L_0$, $\kappa_m = 5.92/l_0$, and L_0 and l_0 refer to the outer scale and inner scale. Note that based on the Kolmogorov theory, L_0 is the largest eddy size before the energy is injected into a region and l_0 is the smallest eddy size before energy is dissipated into heat [34]. After substituting (9) into (8) and taking some approximations, the wave structure function simplifies to [21]

$$D(\rho,L) = \begin{cases} 1.09 C_n^2 k^2 L l_0^{-1/3} \rho^2 [1 - 0.72(\kappa_0 l_0)^{1/3}], \rho \ll l_0, \\ 1.09 C_n^2 k^2 L \rho^{5/3} [1 - 0.72(\kappa_0 \rho)^{1/3}], \quad \rho \gg l_0. \end{cases} \tag{10}$$

Substituting (10) into (7) yields to

$$E[\gamma^2] = \begin{cases} 1.09 C_n^2 L l_0^{-1/3} [1 - 0.72(\kappa_0 l_0)^{1/3}] \ , \ d \ll l_0, \\ 1.09 C_n^2 L d^{-1/3} [1 - 0.72(\kappa_0 d)^{1/3}] \ , \ d \gg l_0. \end{cases} \tag{11}$$

If we further assume that $d \gg l_0$ and ignore both inner scale and outer scale effects [35], [36], i.e., $L_0 = \infty$ and $l_0 = 0$, the second moment of turbulence-induced AOA fluctuations can be written as [21]

$$E[\gamma^2] = 1.09 C_n^2 L d^{-1/3}. \tag{12}$$

Considering that the atmospheric turbulence is statistically homogeneous and isotropic, both the horizontal and vertical angular deviations caused by turbulence, i.e., γ_h and γ_v, are approximately zero mean Gaussian distributed and the total radial deviation $\gamma = \sqrt{\gamma_h^2 + \gamma_v^2}$ is thus Rayleigh distributed with PDF given by [17], [18]

$$f_\gamma(\gamma) = \frac{\gamma}{\sigma_\gamma^2} \exp\left(\frac{-\gamma^2}{2\sigma_\gamma^2}\right), \tag{13}$$

where the parameter σ_γ^2 refers to the variance of γ_h and γ_v and can be described based on the second moment of γ in (11) as $\sigma_\gamma^2 = E[\gamma^2]/2$. Note that when the turbulence is anisotropic which is out of the scope of this work, the AOA would be Hoyt-distributed [18]. In the presence of turbulence, the position of the optical beam might be deviated randomly from the light-of-sight which is commonly called as beam wander [37]. Thus turbulence introduces both beam misalignment and AOA fluctuations. However, it is shown that the effect of beam wander is negligible especially when divergent beam is employed [2]. Thus in the following discussion, only AOA fluctuations caused by turbulence will be taken into account.

C. Transceiver Vibrations

The transceiver vibrations are introduced by phenomena such as building sways and might significantly limit the performance of FSO systems where an ideal tracking system is not in place. Impairments caused by transceiver vibrations are generally two-folded. Firstly, due to the pointing errors caused by transmitter vibrations, the received Gaussian beam footprint deviates from the centre of the receive aperture, which directly reduces the received signal power. Secondly, the receiver vibrations introduce additional AOA fluctuations which degrade the performance of FSO systems with limited FOV [16]. This effect has been mostly ignored in the literature on terrestrial FSO communication by assuming FOVs of receivers to be very large [13], [14], [38].

For the first impairment which will be thereafter referred as *beam misalignment*, the fraction of the signal power incident on the aperture to the total transmit power denoted by h_p

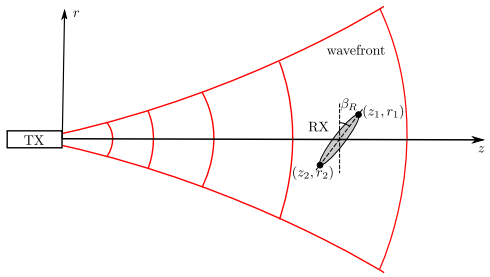

Fig. 2. The angle of arrival in the presence of receiver vibrations.

is proposed to describe the effect of transmitter vibrations on irradiance [13], [24]. Considering the expression of optical field collected by aperture (1), h_p can be expressed as $\int_{\mathcal{A}} |s_r(\mathbf{r})|^2 \mathrm{d}\mathbf{r}/P_t$ where P_t refers to the transmitted optical power and $\mathcal{A} = \pi d^2/4$ is the aperture area. Using the general model proposed in [24], h_p can be approximated as

$$h_p(\beta_T) = A_0 \exp\left(-\frac{2\beta_T^2 L^2}{w_{\mathrm{zeq}}^2}\right), \tag{14}$$

and its PDF can be written as

$$f_{h_p}(h_p) = \frac{r^2}{A_0^{r^2}} {h_p}^{r^2-1} \quad , \quad 0 \le h_p \le A_0, \tag{15}$$

where β_T is the radial angular deviation caused by transmitter pointing errors, A_0 is the fraction of the signal power over the aperture in the absence of pointing errors, $r = w_{\mathrm{zeq}}/2\sigma_s$ is the ratio between the equivalent beam radius at the receiver w_{zeq} and the pointing error displacement standard deviation σ_s. Note that

$$v = \frac{\sqrt{\pi} d}{2\sqrt{2} w_z}, \quad A_0 = [\mathrm{erf}(v)]^2, \quad w_{\mathrm{zeq}}^2 = w_z^2 \frac{\sqrt{\pi}\mathrm{erf}(v)}{2v\exp(-v^2)}, \tag{16}$$

where w_z refers to the beam waist of the Gaussian beam at the receiver plane. In (15), the relationship between β_T and beam displacement at receiver plane s_d (i.e., $s_d = L\beta_T$) is applied which is justified when β_T is small [23]. Therefore, the relationship between the standard deviations of receiver vibration angle and displacement is given by $\sigma_s = L\sigma_{\beta_T}$.

Now we turn to the second impairment, namely, AOA fluctuation caused by receiver vibrations. For far-field communication, a divergent Gaussian beam appears to diverge as a spherical wave which renders the effect of transmitter vibrations on angle of arrival negligible. However, this is not the case for the receiver vibrations as shown in Fig. 2. The phase shift across the receiver aperture is given by $\Delta S = k\Delta l$ where Δl refers to the optical path difference between the two ends of the receiver aperture (i.e., (z_1, r_1) and (z_2, r_2)) as shown in the figure. Using the spherical wave propagation to model the received phase front, the optical path difference Δl can be expressed as

$$\Delta l = \sqrt{z_1^2 + r_1^2} - \sqrt{z_2^2 + r_2^2}, \tag{17}$$

where

$$z_1 = L + \frac{d}{2}\sin\beta_R, \quad r_1 = \frac{d}{2}\cos\beta_R, \tag{18}$$
$$z_2 = L - \frac{d}{2}\sin\beta_R, \quad r_2 = -\frac{d}{2}\cos\beta_R,$$

and the receiver vibration angle is denoted as β_R. Noting that using $L \gg d$ and $\sin(\beta_R) \approx \beta_R$, (17) can be written as $\Delta l \approx \beta_R d$. Recalling the definition of AOA (6), the AOA caused by the receiver vibration can be obtained as $\Delta S/(kd) = k\Delta l/(kd) \approx \beta_R$, i.e., equal to the receiver vibration angle. Thereafter, this AOA will be referred as *vibration-induced AOA*. As commonly assumed in literature [13], [26], [39], we employ the assumption that the angular deviations in vertical and horizontal direction caused by building sways, i.e., $\beta_{R,v}$ and $\beta_{R,h}$, respectively, are independent and identically distributed (iid) zero mean Gaussian random variables with variance σ_β^2. Thus β_R is Rayleigh distributed with the scale parameter σ_β. In addition, considering that the distance between transmitter and receiver is on the order of several kilometres, it is reasonable to assume that the transmitter and receiver vibration angles, i.e., β_T and β_R, are independent and identically distributed.

D. Fading Caused by AOA Fluctuations

As explained in Section II-B and Section II-C, both atmospheric turbulence and receiver vibrations make contributions to the radial angular fluctuations. In particular, turbulence-induced AOA fluctuation is introduced by phase distortions caused by atmospheric turbulence whereas vibration-induced AOA fluctuation results from receiver vibrations. Therefore, it is reasonable to assume that these two effects are independent. The total vertical and horizontal angular deviations can be respectively written as

$$\varepsilon_v = \beta_{R,v} + \gamma_v, \quad \varepsilon_h = \beta_{R,h} + \gamma_h, \tag{19}$$

where $\beta_{R,v}$ and $\beta_{R,h}$ are iid zero mean Gaussian distributed as well as γ_v and γ_h. Therefore, the total radial AOA ε given by $\varepsilon = \sqrt{\varepsilon_v^2 + \varepsilon_h^2}$ remain Rayleigh distributed as

$$f_\varepsilon(\varepsilon) = \frac{\varepsilon}{\sigma_\beta^2 + \sigma_\gamma^2} \exp\left[\frac{-\varepsilon^2}{2\left(\sigma_\beta^2 + \sigma_\gamma^2\right)}\right]. \tag{20}$$

In practical FSO systems, in order to collect sufficient optical power, an aperture much larger than the size of the photodetector is employed on receiver plane and an optical lens is applied to focus the incident optical field to the focal plane where the small photodetector is located. The amount of received signal power is determined by the overlap between the focused field pattern and the photodetector area. Any power outside the photodetector area cannot be detected even though the aperture has collected the optical field [40]. Under the Fraunhofer approximation, AOA fluctuations generate shifted diffracted patterns which attenuate the amount of collected signal power by reducing the overlap area. Therefore, for practical FSO receivers with limited FOV, this random attenuation (i.e., fading) introduced by AOA fluctuations needs to be taken into account.

Since the received optical field over the receiver aperture can be considered a tilt plane as mentioned above, the optical field collected by receiver aperture (1) can be rewritten as $x(\mathbf{r}) = s_r(\mathbf{r})e^{\chi+j\mathbf{k}\cdot\mathbf{r}}$ [41], where $\mathbf{k}$ is the wave vector passing through the origin of the receiver aperture in the direction of the optical propagation with a magnitude equal to the wave number as defined before. Using the small angle approximation, the coordinates of $\mathbf{k}$ can be expressed as $(k\varepsilon_h, k\varepsilon_v)$, hence $x(\mathbf{r})$ can be written as [29]

$$x(\mathbf{r}) = s_r(\mathbf{r})\, e^{\chi} \exp\left[jk\left(r_x\varepsilon_h + r_y\varepsilon_v\right)\right]. \tag{21}$$

For a thin focusing lens, the diffracted pattern on the detector plane can be described as the Fourier transform of $x(\mathbf{r})$ [42]. Therefore, the intensity of diffracted pattern at the detector plane can be expressed as the well-known Airy pattern for circular apertures with a displacement vector $\mathbf{q_0} = (f_c\varepsilon_h, f_c\varepsilon_v)$ [41], i.e.,

$$I(\mathbf{q}-\mathbf{q_0}) = \frac{h_a h_p P_t \mathcal{A}}{\lambda^2 f_c^2}\left[\frac{2J_1\left(\pi d|\mathbf{q}-\mathbf{q_0}|/\lambda f_c\right)}{\pi d|\mathbf{q}-\mathbf{q_0}|/\lambda f_c}\right]^2, \tag{22}$$

where $\mathbf{q} = (x, y)$ represents vector position in the detector plane, f_c refers to the focal length of the lens, $J_1(\cdot)$ is Bessel function of the first kind and $h_a h_p P_t$ is the total power incident on the receive aperture (i.e., $\int_{\mathcal{A}} |x(\mathbf{r})|^2 \mathrm{d}\mathbf{r} = h_a h_p P_t$) in which the power loss introduced by both log-amplitude fluctuation and beam misalignment is taken into account. In deriving (22), the intensity of the received optical field is approximated as almost constant within the aperture as the aperture is small compared to the received beam width. In practice, most lenses are designed with a focal length approximately equal to the the diameter of aperture [29], i.e., $f_c = d$, thus the signal power collected by the detector with respect to the displacement vector $\mathbf{q_0}$ is

$$P_r = \int_{\mathcal{A}_d} I(\mathbf{q}-\mathbf{q_0})\mathrm{d}\mathbf{q}, \tag{23}$$

where $\mathcal{A}_d$ refers to the detector area. Considering a circular detector, P_r only depends on the radial displacement $|\mathbf{q_0}| = d\varepsilon$. Without loss of generality, we assume that the displacement of Airy pattern is in x-axis of detector plane and by substituting (22) into (23) the received signal power can be expressed as

$$P_r = \frac{h_a h_p P_t \mathcal{A}}{\lambda^2 d^2}\int_{-a}^{a}\int_{-\xi}^{\xi}\left[\frac{2J_1\left(\frac{\pi}{\lambda}\sqrt{(x-d\varepsilon)^2+y^2}\right)}{\frac{\pi}{\lambda}\sqrt{(x-d\varepsilon)^2+y^2}}\right]^2 \mathrm{d}y\mathrm{d}x, \tag{24}$$

where a is the radius of the detector and $\xi = \sqrt{a^2-x^2}$. The receiver FOV solid angle Ω_{FOV} is defined as $\Omega_{\mathrm{FOV}} = D\Omega_{\mathrm{DL}}$ where Ω_{DL} is the diffraction-limited solid angle and the ratio D is greater than or equal to 1. Therefore, the relationship between the receiver FOV angle and diffraction-limited angle is given by $\theta_{\mathrm{FOV}} = \sqrt{D}\theta_{\mathrm{DL}}$. Noting that since $\theta_{\mathrm{DL}} = 2\lambda/d$, the receiver FOV angle is given by $\theta_{\mathrm{FOV}} \approx 2\sqrt{D}\lambda/d$. The FOV angle can be also expressed in terms of the detector radius a and the focal length as $\theta_{\mathrm{FOV}} \approx 2a/d$ yielding $a = \sqrt{D}\lambda$ [29].

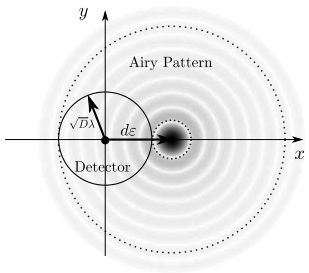

Fig. 3. The power collected by the detector when the centre of Airy pattern is outside the detector area. The detector radius is $\sqrt{D}\lambda$ and the Airy pattern displacement is $d\varepsilon$.

Denote the fading introduced by AOA fluctuations as the fraction of power collected by the detector P_r to the power incident on the aperture $h_a h_p P_t$, i.e,

$$h_{aoa}(\varepsilon) = \frac{\mathcal{A}}{\lambda^2 d^2}\int_{-a}^{a}\int_{-\xi}^{\xi}\left[\frac{2J_1\left(\frac{\pi}{\lambda}\sqrt{(x-d\varepsilon)^2+y^2}\right)}{\frac{\pi}{\lambda}\sqrt{(x-d\varepsilon)^2+y^2}}\right]^2 \mathrm{d}y\mathrm{d}x. \tag{25}$$

The received optical power can then be expressed as

$$P_r = h_a h_p h_{aoa} P_t. \tag{26}$$

For large $\mathcal{A}_d$ which is commonly assumed in previous works, according to (25) one can calculate that $h_{aoa} = 1$. Unfortunately (25) cannot be solved analytically. In order to get an analytical expression for h_{aoa}, some approximations should be thus applied. The common assumption used in the literature is that when the AOA of the signal is outside the receiver FOV, no signal power is detected and the maximum signal power is collected otherwise [13], [19], [21], i.e.,

$$h_{aoa}(\varepsilon) \approx \begin{cases} h_{aoa}(0)\,, & 0 \le \varepsilon \le \sqrt{D}\lambda/d, \\ 0, & \varepsilon > \sqrt{D}\lambda/d. \end{cases} \tag{27}$$

Consider a circle with radius ζ centred at the center of the Airy pattern. The fraction of the power contained in this circle to the power incident on the aperture is given by [41]

$$\mathcal{W}(\zeta) = 1 - J_0^2\left(\frac{\pi\zeta}{\lambda}\right) - J_1^2\left(\frac{\pi\zeta}{\lambda}\right). \tag{28}$$

Therefore, in (27) when the signal is within the FOV of the receiver $h_{aoa}(0) = \mathcal{W}(\sqrt{D}\lambda)$. Note that despite the assumption in the approximation above, significant signal power may still be collected at high transmit power regime even though the AOA is outside receiver FOV. This power is collected because of the existence of side lobes of Airy pattern inside the detector area. Here, we enhance the above approximation by determining the detected power when AOA is outside receiver FOV, i.e., the centre of Airy pattern is outside the detector area as illustrated in Fig. 3. We first use (28) to calculate the signal power contained in the ring circumscribing the detector circle by subtracting the power contained in the its inner circle (with radius $d\varepsilon - \sqrt{D}\lambda$) from that of its outer circle (with radius $d\varepsilon + \sqrt{D}\lambda$). The power collected by the detector is then approximated as a fraction α of the power contained in the ring where the fraction $\alpha = \sqrt{D}\lambda/4d\varepsilon$ is considered to be

the ratio of the area of the detector to that of the ring. Thus $h_{aoa}(\varepsilon)$ is expressed as

$$h_{aoa}(\varepsilon) \approx \alpha \left[\mathcal{W}(d\varepsilon + \sqrt{D}\lambda) - \mathcal{W}(d\varepsilon - \sqrt{D}\lambda)\right], \quad (29)$$

for $\varepsilon > \sqrt{D}\lambda/d$. In summary, the fading introduced by AOA fluctuations for receiver with limited detector size can be expressed as

$$h_{aoa}(\varepsilon) = \begin{cases} \mathcal{W}(\sqrt{D}\lambda), & 0 \le \varepsilon \le \sqrt{D}\lambda/d, \\ \alpha \left[\mathcal{W}(d\varepsilon + \sqrt{D}\lambda) - \mathcal{W}(d\varepsilon - \sqrt{D}\lambda)\right], & \text{o/w.} \end{cases} \quad (30)$$

III. Outage Performance Analysis

The average number of transmitted signal photons in one bit period can be expressed as $N_s = \tau E[P_t]/h_{\rm Pk}\nu$ where τ is the bit time, ν is the frequency of laser and $h_{\rm Pk}$ is the Planck's constant. Taking the channel fadings introduced in Section II into account and considering the expression of received optical power (26), the average number of received signal photons in a bit period is then given by $\eta h_a h_p h_{aoa} N_s$, where η refers to the quantum efficiency of photodetector which is set to unity thereafter for sake of simplicity. The power attenuation due to absorption and scattering which is weather-dependent is also normalized to unity due to the fixed link distance.

In optical communications, the data rates are very high and thus the channel coherence time of few milliseconds is very long compared to the bit period which means that a large number of bits would be affected during poor channel states. Therefore, outage probability is an appropriate metric to evaluate the performance of FSO systems in the presence of atmospheric turbulence and other slow-varying random impairments [6], [21]. Outage probability is defined as the probability when the instantaneous bit error probability (BEP) is bigger than a threshold BEP that is required to guarantee an essentially error-free transmission when forward error correction is applied and is given by

$$P_{\rm out} = \Pr\left\{P_e > P_e^{\rm th}\right\}, \quad (31)$$

A. Direct Detection

Let us first consider the performance of the receiver with direct detection. Here BPPM is employed as the modulation scheme. Note that in the two time slots of a bit period, only one contains the signal pulse, thus all of the signal photons N_s are concentrated in only one half bit time. Using the Poisson detection model for the photodetector, an approximate expression of the BEP for diffraction-limited receiver is given by (29) in [10]. However, the derivation in [10] ignores angular fluctuations caused by turbulence and transceiver vibrations. In fact, in most of practical systems, the receiver FOV is larger than the diffraction-limited FOV in order to compensate for these fluctuations. Here we consider a general scenario where the receiver FOV is D times bigger than diffraction-limited FOV as mentioned before. The average count of background noise photons per bit time is then given by [29]

$$N_n' = \frac{\Omega_{\rm FOV}}{\Omega_{\rm DL}} N_n = D N_n, \quad (32)$$

where N_n refers to the average background noise photon counts per symbol per bit period for diffraction-limited receiver. Using the method proposed in [10] and considering both turbulence and transceiver vibrations, the BEP for shot-noise limited receiver with direct detection can be written as

$$P_e = \exp\left[-\left(\sqrt{h_a h_p h_{aoa} N_s + \frac{DN_n}{2}} - \sqrt{\frac{DN_n}{2}}\right)^2\right]. \quad (33)$$

Instantaneous h_p and h_{aoa} are determined by transmitter pointing error angle β_T and angle-of-arrival ε respectively as in (14) and (30). Thus, the BEP (33) is inherently dependent on both β_T and ε. Substituting (33) into (31) and after some mathematical manipulation, $P_{\rm out}$ can be expressed as

$$P_{\rm out} = \Pr\left\{h_a h_p h_{aoa} < \frac{\theta_{\rm th} + \sqrt{2DN_n\theta_{\rm th}}}{N_s}\right\}, \quad (34)$$

where $\theta_{\rm th}$ is the exponent of the error probability threshold, i.e., $P_e^{\rm th} = e^{-\theta_{\rm th}}$. Since h_a, h_p and h_{aoa} are independent random variables, (34) can be expressed as

$$P_{\rm out} = \int_0^{+\infty} \Pr\left\{h_a h_p < \frac{\theta_{\rm th} + \sqrt{2DN_n\theta_{\rm th}}}{N_s h_{aoa}(\varepsilon)}\right\} f_\varepsilon(\varepsilon){\rm d}\varepsilon, \quad (35)$$

where $f_\varepsilon(\varepsilon)$ is the PDF of AOA given in (20). If we denote $h_{ap} = h_a h_p$, its PDF is given by [24]

$$f_{h_{ap}}(h_{ap}) = \frac{r^2 h_{ap}^{r^2-1} e^{2r^2\sigma_\chi^2 + 2r^4\sigma_\chi^2}}{2A_0^{r^2}} \,{\rm erfc}\left(\frac{\mu + \ln\frac{h_{ap}}{A_0}}{\sqrt{8}\sigma_\chi}\right), \quad (36)$$

where $\mu = 2\sigma_\chi^2(1 + 2r^2)$ and r is given in (15). After some algebraic manipulations, its CDF can be written as

$$\begin{aligned} \mathcal{F}(x) =& \frac{1}{2}\exp\left(r^2 \ln\frac{x}{A_0} + 2\sigma_\chi^2 r^2 + 2\sigma_\chi^2 r^4\right) \quad (37) \\ & \times {\rm erfc}\left[\frac{\ln\frac{x}{A_0} + \mu}{\sqrt{8}\sigma_\chi}\right] + \frac{1}{2}{\rm erfc}\left(\frac{-\ln\frac{x}{A_0} - 2\sigma_\chi^2}{\sqrt{8}\sigma_\chi}\right), \end{aligned}$$

for $x \in [0, +\infty]$. Thus (35) can be simplified as

$$P_{\rm out} = \int_0^{+\infty} \mathcal{F}\left[\frac{\theta_{\rm th} + \sqrt{2DN_n\theta_{\rm th}}}{N_s h_{aoa}(\varepsilon)}\right] f_\varepsilon(\varepsilon){\rm d}\varepsilon. \quad (38)$$

Applying the expression of h_{aoa} in (30), the integral (38) can be divided into two terms

$$\begin{aligned} P_{\rm out} =& \int_0^{\sqrt{D}\lambda/d} \mathcal{F}\left[\frac{\theta_{\rm th} + \sqrt{2DN_n\theta_{\rm th}}}{N_s \mathcal{W}(\sqrt{D}\lambda)}\right] f_\varepsilon(\varepsilon){\rm d}\varepsilon \quad (39) \\ & + \int_{\sqrt{D}\lambda/d}^{+\infty} \mathcal{F}\left[\frac{\theta_{\rm th} + \sqrt{2DN_n\theta_{\rm th}}}{N_s h_{aoa}(\varepsilon)}\right] f_\varepsilon(\varepsilon){\rm d}\varepsilon, \end{aligned}$$

where the first term (thereafter denoted by $P_{\rm out,in}$) refers to the outage probability when AOA is within the receiver FOV and the second integral (denoted by $P_{\rm out,out}$) refers to that when AOA is outside the receiver FOV. Considering the

CDF of ε which is Rayleigh distributed, $P_{\text{out,in}}$ can be solved analytically as

$$P_{\text{out,in}} = \left[1 - \exp\left(-\frac{D\lambda^2}{2d^2\sigma_\varepsilon^2}\right)\right] \mathcal{F}\left[\frac{\theta_{\text{th}} + \sqrt{2DN_n\theta_{\text{th}}}}{N_s\mathcal{W}(\sqrt{D}\lambda)}\right]. \tag{40}$$

On the other hand, by substituting (20) and (30) into the second integral in (39), $P_{\text{out,out}}$ can be solved numerically.

In the presence of both beam misalignment and AOA fluctuations, two trade-offs exist. The first trade-off resulting from beam misalignment has already been investigated in [24]. Assuming that the received beam radius w_z can be adjusted, we can increase the average overlap area between the receiver aperture and the beam by enlarging w_z thereby reducing the power loss caused by transmitter pointing errors. However, increasing w_z will in turn reduce the average intensity of the beam which successively decreases the received signal power. Thus an optimal w_z can be determined to minimize the overall outage probability. Secondly, narrow FOV is required for FSO receivers to reduce collected background noise (32) [10]. However, in the presence of AOA fluctuations, a narrow FOV also reduces the amount of detected signal power (30). This trade-off implies that an optimal FOV or optimal D value that minimizes the outage probability (39) should exist. In order to find the optimal FOV for direct detection, we minimize (39) with respect to D numerically in the simulation, since an analytical solution of this optimization problem is not available.

B. Coherent Detection

For coherent detection, we employ homodyne detection and BPSK is used as the modulation scheme. Note that, unlike direct detection, coherent detection is quite sensitive to the AOA fluctuations and the employment of an active tracking system is essential in order to establish spatial phase match between the received optical field and the field generated by the local laser [29]. We firstly assume that an ideal AOA tracking system is employed in the receiver so that the received signal phasefront can be estimated and perfectly compensated, i.e., $\theta(\mathbf{r}) = 0$, thus there is no misalignment between received field and local fields in the focal plane so that an idealized coherent detection is achieved. In Section IV, we extend our analysis to more practical coherent receivers with imperfect phase tracking.

The BEP of coherent detection degraded by log-amplitude fluctuations is given in [43]. Invoking the power loss introduced by limited detector area h_{aoa} in (30), for coherent detection with perfect phasefront compensation, i.e., $\varepsilon = 0$, both the received signal and the background noise are degraded by a power loss factor $h_{aoa}(0) = \mathcal{W}(\sqrt{D}\lambda)$. Using the same strategy employed in [43] and considering effect of beam misalignment and limited detector size, the BEP can be written as

$$P_e = \frac{1}{2}\exp\left[-\frac{2h_a h_p \mathcal{W}(\sqrt{D}\lambda)N_s}{1 + \mathcal{W}(\sqrt{D}\lambda)N_n}\right]. \tag{41}$$

For large detector plane, $\mathcal{W}(\sqrt{D}\lambda)$ approaches to unity and the effect of limited detector size is negligible. From (41) one can see that for coherent detection, only one background noise mode will be finally seen by the receiver no matter how large the size of the receiver FOV is [29]. The corresponding P_{out} is thus given by

$$P_{\text{out}} = \Pr\left\{h_a h_p < \frac{(\theta_{\text{th}} - \ln 2)\left[1 + \mathcal{W}(\sqrt{D}\lambda)N_n\right]}{2\mathcal{W}(\sqrt{D}\lambda)N_s}\right\}. \tag{42}$$

Recalling the CDF of h_{ap} in (37), this outage probability can be expressed analytically as

$$P_{\text{out}} = \mathcal{F}\left\{\frac{(\theta_{\text{th}} - \ln 2)\left[1 + \mathcal{W}(\sqrt{D}\lambda)N_n\right]}{2\mathcal{W}(\sqrt{D}\lambda)N_s}\right\}. \tag{43}$$

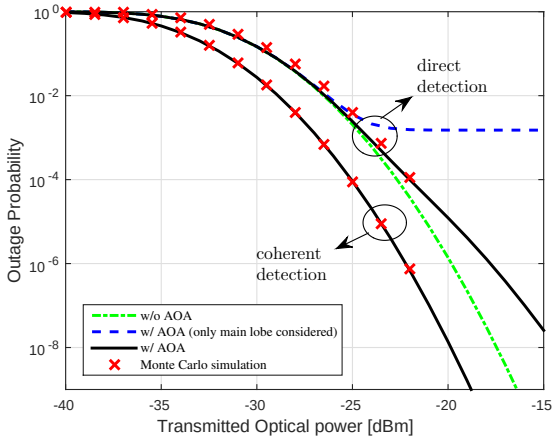

Fig. 4. Outage probability vs. transmitted optical power for diffraction-limited receiver in the absence of transceiver vibrations. (AOA: turbulence-induced angle-of-arrival fluctuations). Perfect AOA tracking system is employed for coherent detection.

C. Results and Discussions

In the following, we will provide simulation results to the performance of FSO communication systems with limited FOV. We set the propagation distance $L = 1$ km, wavelength $\lambda = 1550$ nm, error probability threshold $P_e^{\text{th}} = 1 \times 10^{-4}$, the refractive index structure constant $C_n^2 = 5 \times 10^{-14}\,\text{m}^{-2/3}$ and the data rate as 1 Gb/s. The average count of background noise photons per symbol per spatial mode is $N_n = 1$ [10]. The log-amplitude variance σ_χ^2 can be determined by (3) and using parameters above we can get $\sigma_\chi^2 \approx 0.1$ which corresponds to a weak turbulence condition. The receiver aperture diameter is also assumed as $d = 5$ cm which is smaller than the coherence length of turbulence in the underlying FSO channel described by parameters above. The normalized beam width and the normalized jitter standard deviation are $w_z/d = 10$ and $\sigma_s/d = 2$, respectively [24].

1) In the absence of transceiver vibrations: If the effect of transceiver vibrations is negligible, i.e., $\sigma_s = \sigma_\beta = 0$, the system is impaired by log-amplitude fluctuations as well as turbulence-induced AOA fluctuations. Fig. 4 presents the performance of diffraction-limited receivers for this scenario. In

the literature on terrestrial FSO communication, the effects of AOA fluctuations are normally ignored, however, as presented in Fig. 4 for direct detection the performance is significantly degraded by AOA fluctuations and with the increase of the transmitted power, the degradation becomes even stronger. For example, at $P_{\text{out}} = 10^{-5}$, 1.4 dB degradation is introduced. However, at $P_{\text{out}} = 10^{-7}$, it increases to 2.6 dB. As mentioned in Section II-D, some previous works only take into account the main lobe of Airy pattern to determine signal detection at a limited-FOV FSO receiver as described by (27). Under such simplified assumption, an analytical expression for outage probability can be easily achieved by substituting (27) into (38) [21]. However, it can be observed from Fig. 4 that in this case an unreasonable outage floor will appear in high transmit power regime. With the increase of P_t, the outage performance flattens rather than decreasing exponentially at a fixed value 0.0015 which is the probability when the AOA is inside FOV. This issue happens since when transmit power is large enough, the power contained in the side lobes of Airy pattern is non-negligible which means that we can still collect a significant amount of power even though the AOA is outside the receiver FOV. In terms of coherent detection with perfect AOA tracking, the degradation of AOA fluctuations is negligible.

For diffraction-limited receiver the performance improvement of coherent detection over direct detection in the absence of AOA fluctuations is about 2 dB as presented in Fig. 4, which corresponds to the conclusion in [10]. However, according to our simulation results, the advantage of coherent detection are underestimated. When AOA fluctuations are considered we can get more improvement by employing coherent detection. For instance, in order to achieve $P_{\text{out}} = 10^{-6}$, -17.8 dBm transmit power is required for direct detection. However, for coherent detection, the corresponding transmit power is only -22.2 dBm. Thus 4.4 dB power gain can be achieved. Note that with the increase of transmit power, the performance gap between direct and coherent detection also increases. This is because coherent detection has higher sensitivity, the power required for reliable communication is smaller than that of direct detection. Finally, note that the Monte Carlo simulation, which is based on precise calculation of the received optical power using the complete Bessel form of Airy pattern as in (24), shows that our approximated analytical expressions are very accurate.

Fig. 5 shows the outage performance with various receiver FOV. One can see that, for direct detection, by enlarging the FOV from diffraction-limited ($D = 1$) to $D = 4$, the performance is degraded in low P_t regime. Because in this regime the negative effect of added background noise is so strong and smaller FOV which has less received background noise performs better. However in high P_t regime, the performance of receiver with $D = 4$ becomes better than diffraction-limited receiver. The reason is that with the increase of P_t, the ratio of the number of background noise photons per bit to the number of signal photons per bit becomes smaller and the degradation caused by background noise decreases. Thus bigger FOV which has higher probability of receiving more signal power has better performance. If we further increase

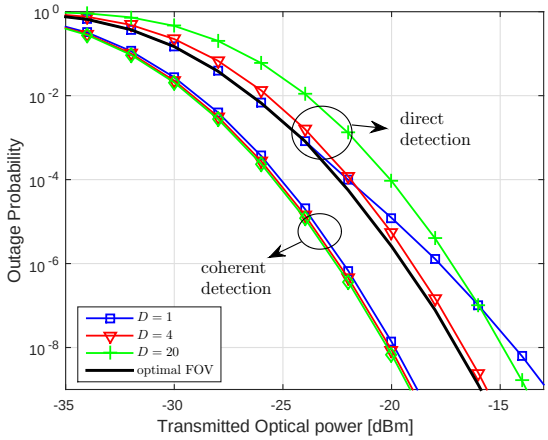

Fig. 5. Outage probability vs. transmitted optical power for receivers with different FOV in the absence of transceiver vibrations. Perfect AOA tracking system is employed for coherent detection.

the FOV, i.e., $D = 20$, the performance is worse than that of diffraction-limited receiver because of the large amount of background noise received. Due to the trade-off between received signal power and background noise, an optimal FOV and correspondingly an optimal value of D can be calculated that minimizes the outage probability (39) for each specific transmit optical power as shown in Fig. 5. Note that the optimal D value increases with the increase of transmitted optical power. However, even using optimal receiver FOV, the performance of direct detection is still outperformed by coherent detection. Also note that coherent detection always benefits from larger FOV as shown in Fig. 5 due to higher signal power reception while the collected background noise remains fixed.

2) In the presence of transceiver vibrations: In this section, the performance of receivers with limited FOV in the presence of transceiver vibrations is considered. Thus besides turbulence-induced AOA fluctuations, the effects of beam misalignment and vibration-induced AOA fluctuations are also included. Fig. 6 plots the corresponding outage probability. For direct detection, the outage probability firstly decreases exponentially. However, with the increase of transmit power, the slope then decreases. Since with the increase of P_t, the outage occurs when AOA is in the FOV turns negligible, however the power contains in side lobes of Airy pattern is still not big enough to make contributions to the decrease of the outage probability. With the continuous increase of P_t, the slope starts to slowly increase again due to the power addition in side lobes when AOA is out of the receiver FOV. Since the fraction of power in side lobes is much smaller than that in main lobe, the decrease of outage probability with respect to P_t in high P_t regime is much slower than that in small P_t regime.

By comparing with the case in the absence of beam misalignment and AOA fluctuations, one can see the significant degradation caused by these adverse effects especially in high P_t regime. When the system is operated to satisfy $P_{\text{out}} = 10^{-4}$, -17 dBm transmit power is required in the ab-

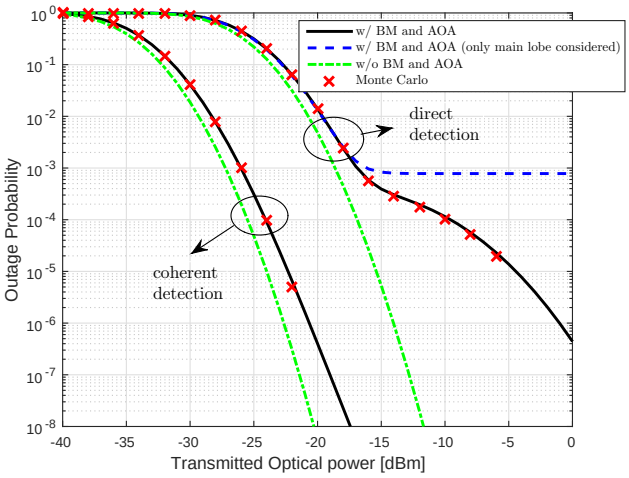

Fig. 6. Outage probability vs. transmitted optical power for FSO receiver in the presence of transceiver vibrations, $D = 150$ (BM: beam misalignment). Perfect AOA tracking system is employed for coherent detection.

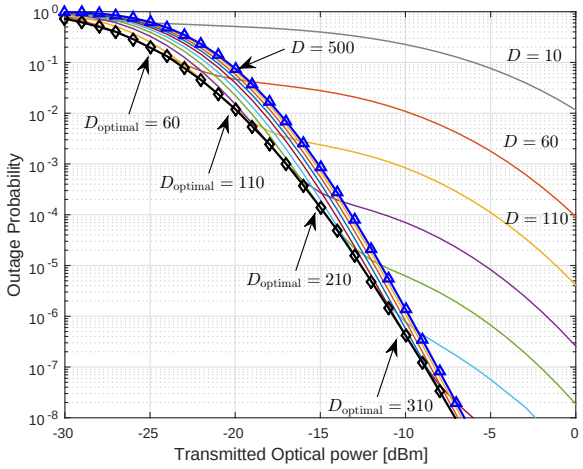

Fig. 7. Outage probability vs. transmitted optical power for receiver with various FOV in the presence of transceiver vibrations.

sence of beam misalignment and AOA fluctuations. However, considering these effects, the required transmit power increases to -10 dBm. Thus 7 dB degradation is observed. In terms of coherent detection, since perfect phasefront compensation is assumed, the effect of AOA fluctuations is negligible and the system is only degraded by beam misalignment. For example, at $P_{\text{out}} = 10^{-8}$, 2.5 dB degradation is introduced. Furthermore, we can observe the significant improvement of coherent detection over direct detection in the presence of transceiver vibrations. For instance, when $P_{\text{out}} = 10^{-4}$, 14 dB gain can be achieved using coherent detection. Finally, we should emphasize that the Monte Carlo simulation based on precise modelling of Airy pattern demonstrates an excellent match with our analytical results.

In Section III-A, it is mentioned that both optimal beam width and receiver FOV can be determined in the presence of transceiver vibrations. Since optimal beam width has been thoroughly investigated in [24], in this work only optimal FOV will be considered. In Fig. 7, we plot the performance of receiver with various FOV ranges from $D = 10$ to $D = 500$ in discrete steps of $\Delta D = 50$ which are typical values for high-speed FSO communication systems [16]. We can still see that when P_t is small, receiver with smaller FOV has better performance and with the increase of P_t, higher FOV is preferable. For each specific P_t, an optimal FOV can be selected to minimize the outage performance and its performance is also shown in Fig. 7. For example, compared to the receiver with $D = 500$ which corresponds to a photodetector with a diameter of 70 μm, about 2 dB gain can be realized to satisfy $P_{\text{out}} = 10^{-3}$ using the optimal FOV.

IV. AOA Tracking for Coherent Detection

A. Field Misalignment

The coherent detection receiver discussed so far is an ideal one based on the assumption that the signal field and local laser field are perfectly matched. In order to achieve ideal coherent detection, perfect angle-of-arrival estimation and compensation are required. Since the receive aperture size is smaller than coherence length, the received optical phasefront seen by the aperture is assumed to be a tilted plane where the tilted angle is random and is defined by AOA fluctuations caused by turbulence and receiver vibrations. In the absence of AOA fluctuations, we set that the AOAs of incoming signal and local laser are the same and normal to the aperture plane so that perfect phase alignment is achieved. In the presence of AOA fluctuations, the misalignment of the two Airy patterns in the focal plane will degrade the receiver performance. It has been shown that this misalignment between the two Airy patterns results in a multiplying loss factor on the received signal amplitude which is given by [29]

$$L_H = \frac{1}{\mathcal{A}} \left| \int_{\mathcal{A}_d} \phi_s(\mathbf{q}) \phi_L^*(\mathbf{q}) \, \mathrm{d}\mathbf{q} \right|, \tag{44}$$

where $\mathcal{A}$ and $\mathcal{A}_d$ denote the aperture area and detector area respectively, $\mathbf{q}$ is a position vector in the detector plane and $\phi_s(\mathbf{q})$ and $\phi_L(\mathbf{q})$ refer to the Airy patterns of the signal and local laser, respectively. Note that L_H is defined as the amplitude loss factor, thus the received photon count is actually multiplied by a loss factor L_H^2 [29]. We assume that the two Airy patterns are identical in shape, phase and polarization, however, they may not overlap perfectly because of AOA deviation of the received signal. If circular aperture is employed, $\phi_s(\mathbf{q})$ and $\phi_L(\mathbf{q})$ are given by [29]

$$\phi_s(\mathbf{q} - \mathbf{q_0}) = \frac{2\Gamma(\mathbf{q})\mathcal{A}}{\lambda f_c} \frac{J_1\left(\pi d|\mathbf{q} - \mathbf{q_0}|/\lambda f_c\right)}{\pi d|\mathbf{q} - \mathbf{q_0}|/\lambda f_c}, \tag{45}$$

$$\phi_L(\mathbf{q}) = \frac{2\Gamma(\mathbf{q})\mathcal{A}}{\lambda f_c} \frac{J_1\left(\pi d|\mathbf{q}|/\lambda f_c\right)}{\pi d|\mathbf{q}|/\lambda f_c}, \tag{46}$$

where again $\mathbf{q_0}$ is the displacement vector and $\Gamma(\mathbf{q})$ is a phase factor which is given by $\Gamma(\mathbf{q}) = -j\exp\left(j\pi|\mathbf{q}|^2/\lambda f_c\right)$.

Substituting (45) and (46) into (44), we get

$$L_H = \frac{4\mathcal{A}}{\lambda^2 f_c^2}\left|\int_{A_d} \frac{J_1\left(\pi d|\mathbf{q}|/\lambda f_c\right)}{\pi d|\mathbf{q}|/\lambda f_c}\,\frac{J_1\left(\pi d|\mathbf{q}-\mathbf{q_0}|/\lambda f_c\right)}{\pi d|\mathbf{q}-\mathbf{q_0}|/\lambda f_c}\mathrm{d}\mathbf{q}\right|, \tag{47}$$

where the property $\Gamma(\mathbf{q})\Gamma^*(\mathbf{q}) = 1$ is applied. Using the identity [29]

$$\int_{\text{plane}} \frac{J_1\left(|\mathbf{q}|\right)}{|\mathbf{q}|}\,\frac{J_1\left(|\mathbf{q}-\mathbf{q_0}|\right)}{|\mathbf{q}-\mathbf{q_0}|}\mathrm{d}\mathbf{q} = \frac{2\pi J_1\left(|\mathbf{q_0}|\right)}{|\mathbf{q_0}|}, \tag{48}$$

and for a relatively big detector area (47) can be approximated as

$$L_H = \left|\frac{2J_1\left(\pi d|\mathbf{q_0}|/\lambda f_c\right)}{\pi d|\mathbf{q_0}|/\lambda f_c}\right|. \tag{49}$$

Substituting $d \approx f_c$ and the mismatch shift in the position of Airy patterns $|\mathbf{q_0}| = d\varepsilon$ into (49), L_H turns to

$$L_H(\varepsilon) = \left|\frac{2J_1\left(\pi d\varepsilon/\lambda\right)}{\pi d\varepsilon/\lambda}\right|. \tag{50}$$

Taking phasefront misalignment into account, for coherent detection the received signal photon count is now given by $h_a h_p h_{aoa}(\varepsilon) L_H^2(\varepsilon) N_s$. From (50) it is easy to see that $L_H^2(\varepsilon)$ is maximized at 1 in the absence of angular deviation, i.e., $\varepsilon = 0$, which means no misalignment between received signal field and local laser field exists. It is known that the width of the main lobe of the Airy pattern is given by 2.44λ. If the main lobes of the two Airy patterns are totally non-overlapped which corresponds to $d\varepsilon \geq 2.44\lambda$, from (50) $L_H^2(\varepsilon) \approx 0$ meaning the performance of coherent detection is strongly degraded. Thus coherent detection is quite sensitive to AOA fluctuations and even a small angular deviation will cause significant degradation.

Now we investigate the performance for coherent detection without any tracking in the presence of field misalignment caused by AOA fluctuations. The BEP (41) can then expressed as

$$P_e = \frac{1}{2}\exp\left[-\frac{2h_a h_p h_{aoa}(\varepsilon) L_H^2(\varepsilon) N_s}{1+\mathcal{W}(\sqrt{D}\lambda)N_n}\right]. \tag{51}$$

Thus the corresponding outage probability is given by

$$P_{\text{out}} = \Pr\left\{h_a h_p h_{aoa}(\varepsilon) L_H^2(\varepsilon) < \frac{(\theta_{\text{th}} - \ln 2)\left[1+\mathcal{W}(\sqrt{D}\lambda)N_n\right]}{2N_s}\right\}. \tag{52}$$

The probability (52) can be calculated numerically using Monte Carlo simulation.

B. AOA Tracking using Quadrant Detector

In order to make sure that the Airy patterns of the signal the local laser are perfectly aligned, an AOA tracking system should be employed in the receiver. In a typical tracking system, beam-steering device and tracking sensor are two principle elements. Beam-steering device such as tip/tilt mirror is used to adjust and control the angle-of-arrival of the incoming signal. Tracking sensor on the other hand can estimate the tilted angle of the received wavefront and generate the error-control signal for the beam-steering device. The most commonly used tracking sensor is quadrant detector [44]. Quadrant detector contains four individual photodetectors and each photodetector is followed by a finite time integrator to collect the received signal photons during the integration interval. After focusing the signal field on this sensor, the angular deviation can be easily estimated by properly comparing the outputs of the integrators [45]. However, due to the effect of detector noise, the angular estimation is not perfect. It is concluded that the residual AOA or tracking error after the tracking system ψ is Rayleigh distributed [29]. The scale parameter of this Rayleigh distribution is given by [20]

$$\sigma_\psi = \frac{3\pi}{16}\frac{\lambda/d}{\text{SNR}_\text{v}}, \tag{53}$$

where the voltage signal-to-noise ratio SNR_v is defined as [45]

$$\text{SNR}_\text{v} = \frac{n_s}{\sqrt{(n_s+n_b)2B_L}}, \tag{54}$$

where n_s and n_b refer to the number of the total received signal photons and background photons per second, respectively and B_L is the bandwidth of the loop filter in the tracking system. From (54) we know that a smaller B_L leads to a bigger voltage SNR and thus a better angular estimation. However, the loop bandwidth B_L has to be set big enough to track the time variation of the angular fluctuations.

Noting that N_s refers to average number of transmitted signal photons per bit period, we have $n_s = h_a h_p h_{aoa}(\varepsilon) N_s/\tau$ where τ is the bit period and similarly we have $n_b = DN_n/\tau$. Thus the voltage SNR turns to

$$\text{SNR}_\text{v} = \frac{h_a h_p h_{aoa}(\varepsilon) N_s}{\sqrt{\left(h_a h_p h_{aoa}(\varepsilon) N_s + DN_n\right) 2B_L\tau}}. \tag{55}$$

By substituting (55) into (53), the residual AOA variance after tilt compensation can be calculated. When tracking system is used, the field misalignment loss factor can be written as $L_H(\psi) = \left|2J_1\left(\pi d\psi/\lambda\right)/\pi d\psi/\lambda\right|$ where ψ is Rayleigh distributed with parameter given in (53). Substituting this new misalignment loss factor into (52), the outage performance with tracking system can be calculated.

Fig. 8 shows the outage performance for coherent detection with AOA tracking system. Comparing the performance with perfect and without tracking, it is apparent that phasefront misalignment between incoming signal and local laser can significantly degrade the performance. The performance of the system with AOA tracking subsystem with quadrant sensor is also plotted in Fig. 8. As we can see with the decrease of the loop filter bandwidth, the performance becomes closer to that of the case with perfect AOA tracking due to the decrease of loop noise. Thus it can be concluded that tracking system can significantly reduce the degradation caused by field misalignment for coherent detection in the presence of AOA fluctuations. It is worth mentioning that in our investigation, a small receiver aperture is considered therefore only tilt compensation is enough. However, for a large receiver aperture higher order phase distortions need to be considered and more complicated adaptive optics technique should be applied in order to compensate the received phasefront [11]. Furthermore, phasefront tracking system on the receiver can also be applied

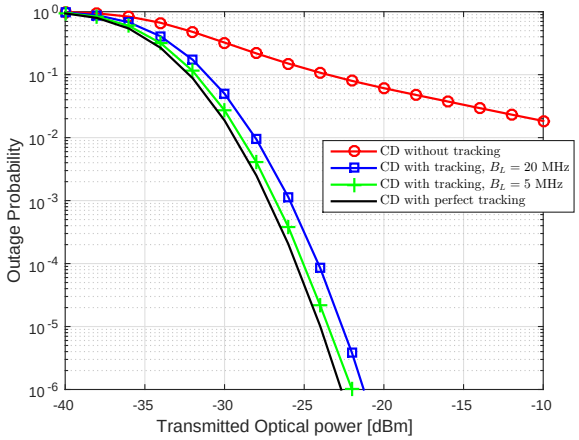

Fig. 8. Outage probability vs. transmitted optical power for coherent detection when tracking system is employed, $D = 500$ and $\sigma_s/d = 0.2$.

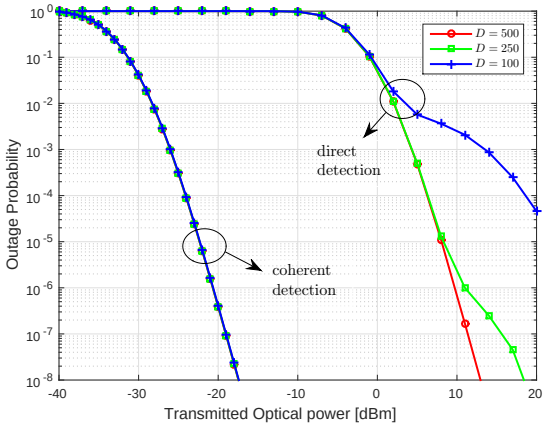

Fig. 9. Outage probability vs. transmitted optical power for thermal-noise-limited receivers with receiver temperature $T^o = 295$ K and local resistance $R_L = 50\ \Omega$.

in direct detection to mitigate the effect of AOA fluctuations. However, due to the cost and complexity restrictions and requirements for system reliability, there is usually a lack of tracking mechanisms in commercial cost-effective FSO links with direct detection [34], [46].

V. Thermal-Noise-Limited Analysis

So far all the discussion is restricted to shot-noise-limited receivers. The main motivation of employing coherent detection is its strong capability of suppressing thermal noise using the added local laser. In this section, the performance of both direct and coherent detections with limited receiver FOV in the presence of angular fluctuations are investigated in thermal-noise-limited regime.

A. Direct Detection

For direct detection with BPPM modulation, when bit "1" is sent which means signal exists only in the first PPM slot, the outputs of the integrators for the two PPM slots in a bit duration τ are given by

$$\begin{aligned} v_1 &= h_a h_p h_{aoa} N_s q + n_1, \\ v_2 &= n_2, \end{aligned} \tag{56}$$

respectively, where q is the electron charge and n_1 and n_2 are the integrated thermal noise Gaussian random variables with zero mean and variance $\sigma_n^2 = N_{0c}\tau/2$. Note that N_{0c} denotes the power spectrum density for thermal noise which is written as [33]

$$N_{0c} = \frac{2\kappa T^o}{R_L}, \tag{57}$$

where κ is Boltzmann's constant, R_L is the load resistance and T^o is the receiver temperature in degrees Kelvin. v_1 can be modelled as a conditional Gaussian random variable given fading parameters with mean and variance $h_a h_p h_{aoa} N_s q$ and σ_n^2, respectively [47]. Meanwhile, the mean and variance of Gaussian random variable v_2 are 0 and σ_n^2, respectively. Thus when the probabilities of sending bit "0" and "1" are equal, the BEP is shown as

$$\begin{aligned} P_e &= \Pr\{v_1 < v_2\} \\ &= \frac{1}{2}\mathrm{erfc}\left(\frac{h_a h_p h_{aoa} N_s q}{2\sigma_n}\right). \end{aligned} \tag{58}$$

The corresponding outage probability is then given by

$$P_{\text{out}} = \Pr\left\{h_a h_p h_{aoa} < \frac{2\sigma_n \mathrm{erfc}^{-1}\left(2P_e^{\text{th}}\right)}{N_s q}\right\}. \tag{59}$$

Using the same method proposed in Section III-A, the expression of outage probability for direct detection can be achieved.

B. Coherent Detection

The BEP for coherent detection with BPSK modulation in the presence of thermal noise is given in [29]. Taking the fadings considered in this work into account, the corresponding BEP can be written as

$$P_e = \frac{1}{2}\mathrm{erfc}\left(\sqrt{\frac{2h_a h_p \mathcal{W}(\sqrt{D}\lambda) N_s}{1 + \mathcal{W}(\sqrt{D}\lambda) N_n + \frac{N_{0c} h_{\text{Pk}} v}{P_L q^2}}}\right), \tag{60}$$

where P_L refers to the power of the local laser and it is assume that optical bandwidth is comparable with electrical bandwidth $B_o\tau = 1$ as in [43] . Note that here we still consider that AOA tracking system is employed so that there is no field misalignment between incoming signal and local laser fields. When a strong local laser is chosen, the thermal noise term in (60) can be removed. If the Chernoff bound for error function $\mathrm{erfc}(x) \approx \exp(-x^2)$ is further applied as in [10], the BEP (60) turns to be the same as (41). Thus shot-noise-limited characteristics are shown for coherent detection when the local laser is strong enough. In the following simulation, the power of the local laser is set high enough so that the outage performance of coherent detection is the same as that for shot-noise-limited receiver.

Fig. 9 shows the outage performance for both direct and coherent detections when the receivers are thermal noise limited.

For direct detection, with the increase of the receiver FOV, the performance is significantly improved on high transmit optical power regime, since receiver with larger FOV has a better capability of reducing the degradation caused by AOA fluctuations. Note that the background radiation is assumed to be negligible compared to thermal noise so that receiver with bigger FOV always outperforms that with smaller FOV. If background radiation is significant, larger FOV might not always perform better due to the added background noise as observed in previous sections. Note that, in commercial FSO systems, smaller photodetectors and therefore smaller FOV should be chosen for higher data rate transmission [16], thus the effect of AOA fluctuations might be significant.

From Fig. 9 it is evident that direct detection is significantly outperformed by coherent detection even when larger FOV is used. For instance, when the outage probability 10^{-7} is satisfied, 11.3 dBm transmitted optical power is required for direct detection with $D = 500$. However, in order to get the same performance, only about -20 dBm optical power is needed if coherent detection is applied resulting in 31.3 dB gain. Therefore, it can be concluded that the advantages of coherent detection become much more obvious for thermal-noise-limited receivers. It is worth mentioning that in practical FSO systems, avalanche photodiodes (APD) can be used to improve the sensitivity of direct detection by up to 10 dB, and thus reduce the performance gap of these two types of detection. Moreover, the imperfect tracking system in coherent detection can further reduce this performance gap.

VI. Conclusion

In this paper, the effects of angular fluctuations on FSO systems are investigated in the presence of both atmospheric turbulence and transceiver vibrations. The performance degradation caused by AOA fluctuations for FOV-limited FSO systems is investigated. It is shown that the impairments of AOA fluctuations are significant especially for smaller FOV receivers which are preferable in commercial FSO systems for higher data rate transmission. Direct detection is strongly outperformed by coherent detection in either shot-noise-limited or thermal-noise-limited regime in the presence of angular fluctuations. However, coherent detection is shown to be more sensitive to AOA fluctuations and in order to achieve better performance AOA tracking is indispensable. For direct detection, narrower FOV can be applied to reduce collected background noise, however, it also reduces the amount of detected signal power when AOA fluctuations are considered. It is demonstrated that optimal FOV leads to significant improvement which can be treated as a novel technique to enhance the communication quality.

References

[1] V. W. S. Chan, "Free-space optical communications," *Journal of Lightwave Technology*, vol. 24, no. 12, pp. 4750–4762, Dec 2006.

[2] L. C. Andrews and R. L. Phillips, *Laser beam propagation through random media*. Bellingham: SPIE press, 2005.

[3] E. Lee and V. W. S. Chan, "Part 1: optical communication over the clear turbulent atmospheric channel using diversity," *IEEE Journal on Selected Areas in Communications*, vol. 22, no. 9, pp. 1896–1906, Nov 2004.

[4] S. Navidpour, M. Uysal, and M. Kavehrad, "BER performance of free-space optical transmission with spatial diversity," *Wireless Communications, IEEE Transactions on*, vol. 6, no. 8, pp. 2813–2819, August 2007.

[5] M. Safari, M. Rad, and M. Uysal, "Multi-hop relaying over the atmospheric poisson channel: Outage analysis and optimization," *IEEE Transactions on Communications*, vol. 60, no. 3, pp. 817–829, March 2012.

[6] M. Safari and M. Uysal, "Relay-assisted free-space optical communication," *IEEE Transactions on Wireless Communications*, vol. 7, no. 12, pp. 5441–5449, December 2008.

[7] M.-A. Khalighi, N. Schwartz, N. Aitamer, and S. Bourennane, "Fading reduction by aperture averaging and spatial diversity in optical wireless systems," *J. Opt. Commun. Netw.*, vol. 1, no. 6, pp. 580–593, Nov 2009.

[8] M. Safari and S. Hranilovic, "Diversity and multiplexing for near-field atmospheric optical communication," *IEEE Transactions on Communications*, vol. 61, no. 5, pp. 1988–1997, May 2013.

[9] V. Vilnrotter and M. Srinivasan, "Adaptive detector arrays for optical communications receivers," *Communications, IEEE Transactions on*, vol. 50, no. 7, pp. 1091–1097, Jul 2002.

[10] E. J. Lee and V. W. Chan, "Diversity coherent and incoherent receivers for free-space optical communication in the presence and absence of interference," *J. Opt. Commun. Netw.*, vol. 1, no. 5, pp. 463–483, Oct 2009.

[11] A. Belmonte and J. M. Khan, "Performance of synchronous optical receivers using atmospheric compensation techniques," *Optics express*, vol. 16, no. 18, pp. 14 151–14 162, Aug 2008.

[12] A. Puryear and V. W. S. Chan, "Coherent optical communication over the turbulent atmosphere with spatial diversity and wavefront predistortion," in *Global Telecommunications Conference, 2009. GLOBECOM 2009. IEEE*, Nov 2009, pp. 1–8.

[13] S. Arnon, "Effects of atmospheric turbulence and building sway on optical wireless-communication systems," *Opt. Lett.*, vol. 28, no. 2, pp. 129–131, Jan 2003.

[14] C. C. Chen and C. S. Gardner, "Impact of random pointing and tracking errors on the design of coherent and incoherent optical intersatellite communication links," *IEEE Transactions on Communications*, vol. 37, no. 3, pp. 252–260, Mar 1989.

[15] D. Kedar and S. Arnon, "Optical wireless communication through fog in the presence of pointing errors," *Appl. Opt.*, vol. 42, no. 24, pp. 4946–4954, Aug 2003.

[16] D. M. Jeganathan and D. P. Ionov, "Multi-gigabits-per-second optical wireless communications," *Optical Crossing, http://www. freespaceoptic. com/WhitePapers/Jeganathan*, vol. 20, p. 20, 2001.

[17] J. I. Davis, "Consideration of atmospheric turbulence in laser systems design," *Appl. Opt.*, vol. 5, no. 1, pp. 139–147, Jan 1966.

[18] P. Beckmann, "Signal degeneration in laser beams propagated through a turbulent atmosphere," *J. Res. Nat. Bureau Standards, 69-A, 629*, vol. 640, 1965.

[19] R. Gagliardi and M. Sheikh, "Pointing error statistics in optical beam tracking," *Aerospace and Electronic Systems, IEEE Transactions on*, vol. AES-16, no. 5, pp. 674–682, Sept 1980.

[20] G. A. Tyler and D. L. Fried, "Image-position error associated with a quadrant detector," *J. Opt. Soc. Am.*, vol. 72, no. 6, pp. 804–808, Jun 1982.

[21] S. Huang and M. Safari, "Free-space optical communication in the presence of atmospheric angular spread," in *2015 IEEE International Conference on Communications (ICC)*, June 2015, pp. 5078–5083.

[22] M. Toyoshima, T. Jono, K. Nakagawa, and A. Yamamoto, "Optimum divergence angle of a Gaussian beam wave in the presence of random jitter in free-space laser communication systems," *J. Opt. Soc. Am. A*, vol. 19, no. 3, pp. 567–571, Mar 2002.

[23] K. Kiasaleh, "On the probability density function of signal intensity in free-space optical communications systems impaired by pointing jitter and turbulence," *Optical Engineering*, vol. 33, no. 11, pp. 3748–3757, 1994.

[24] A. A. Farid and S. Hranilovic, "Outage capacity optimization for free-space optical links with pointing errors," *J. Lightwave Technol.*, vol. 25, no. 7, pp. 1702–1710, Jul 2007.

[25] A. Farid and S. Hranilovic, "Diversity gain and outage probability for MIMO free-space optical links with misalignment," *Communications, IEEE Transactions on*, vol. 60, no. 2, pp. 479–487, February 2012.

[26] H. G. Sandalidis, T. Tsiftsis, and G. K. Karagiannidis, "Optical wireless communications with heterodyne detection over turbulence channels with pointing errors," *J. Lightwave Technol.*, vol. 27, no. 20, pp. 4440–4445, Oct 2009.

[27] I. S. Ansari, M. S. Alouini, and J. Cheng, "Ergodic capacity analysis of free-space optical links with nonzero boresight pointing errors," *IEEE Transactions on Wireless Communications*, vol. 14, no. 8, pp. 4248–4264, Aug 2015.

[28] H. AlQuwaiee, H. C. Yang, and M. Alouini, "On the asymptotic capacity of dual-aperture FSO systems with a generalized pointing error model," *IEEE Transactions on Wireless Communications*, vol. PP, no. 99, pp. 1–1, 2016.

[29] R. M. Gagliardi and S. Karp, *Optical Communications*. Wiley, New York, 1976.

[30] J. Strohbehn and S. Clifford, "Polarization and angle-of-arrival fluctuations for a plane wave propagated through a turbulent medium," *IEEE Transactions on Antennas and Propagation*, vol. 15, no. 3, pp. 416–421, May 1967.

[31] X. Zhu and J. Kahn, "Free-space optical communication through atmospheric turbulence channels," *IEEE Transactions on Communications*, vol. 50, no. 8, pp. 1293–1300, Aug 2002.

[32] W. B. Miller, L. C. Andrews, and J. C. Ricklin, "Log-amplitude variance and wave structure function: a new perspective for Gaussian beams," *J. Opt. Soc. Am. A*, vol. 10, no. 4, pp. 661–672, Apr 1993.

[33] S. Karp, *Optical channels: fibers, clouds, water, and the atmosphere*, ser. Applications of communications theory. Plenum Press, 1988.

[34] M. A. Khalighi and M. Uysal, "Survey on free space optical communication: A communication theory perspective," *IEEE Communications Surveys Tutorials*, vol. 16, no. 4, pp. 2231–2258, Fourthquarter 2014.

[35] J. Anguita, I. Djordjevic, M. Neifeld, and B. Vasic, "Shannon capacities and error-correction codes for optical atmospheric turbulentchannels," *J. Opt. Netw.*, vol. 4, no. 9, pp. 586–601, Sep 2005.

[36] M. A. Al-Habash, L. C. Andrews, and R. L. Phillips, "Mathematical model for the irradiance probability density function of a laser beam propagating through turbulent media," *Optical Engineering*, vol. 40, no. 8, pp. 1554–1562, 2001.

[37] J. H. Churnside and R. J. Lataitis, "Wander of an optical beam in the turbulent atmosphere," *Appl. Opt.*, vol. 29, no. 7, pp. 926–930, Mar 1990.

[38] S. Arnon, "Optimization of urban optical wireless communication systems," *IEEE Transactions on Wireless Communications*, vol. 2, no. 4, pp. 626–629, July 2003.

[39] H. AlQuwaiee, I. S. Ansari, and M. S. Alouini, "On the performance of free-space optical communication systems over double generalized gamma channel," *IEEE Journal on Selected Areas in Communications*, vol. 33, no. 9, pp. 1829–1840, Sept 2015.

[40] T.-H. Ho, S. Trisno, I. I. Smolyaninov, S. D. Milner, and C. C. Davis, "Studies of pointing, acquisition, and tracking of agile optical wireless transceivers for free-space optical communication networks," pp. 147–158, 2004.

[41] M. Born and E. Wolf, *Principles of optics: electromagnetic theory of propagation, interference and diffraction of light*. CUP Archive, 2000.

[42] J. W. Goodman, *Introduction to Fourier optics*. Roberts and Company Publishers, 2005.

[43] E. J. Lee and V. W. S. Chan, "Diversity coherent receivers for optical communication over the clear turbulent atmosphere," in *2007 IEEE International Conference on Communications*, June 2007, pp. 2485–2492.

[44] M. Toyoda, K. Araki, and Y. Suzuki, "Measurement of the characteristics of a quadrant avalanche photodiode and its application to a laser tracking system," *Optical Engineering*, vol. 41, no. 1, pp. 145–149, 2002.

[45] R. Tyson, *Principles of adaptive optics*. CRC Press, 2010.

[46] D. A. Rockwell and G. S. Mecherle, "Optical wireless: low-cost, broadband, optical access," *SONA Communications Corporation*, 2007.

[47] K. Kiasaleh, "Performance of APD-based, PPM free-space optical communication systems in atmospheric turbulence," *IEEE Transactions on Communications*, vol. 53, no. 9, pp. 1455–1461, Sept 2005.